Computer controlled intracavity SHG in a cw ring dye laser

C. M. Marshall, R. E. Stickel, F. B. Dunning, and F. K. Tittel

A tunable computer controlled UV laser spectrometer utilizing intracavity second harmonic generation of a cw ring dye laser is described. The spectrometer yields broadband (~100-GHz) second harmonic outputs of up to 30 mW and narrowband (~100-MHz) single-mode UV outputs of up to 10 mW continuously tunable over intervals of 3200 GHz in the 285–311-nm wavelength range.

Second harmonic generation (SHG) and sum frequency mixing are widely used to generate tunable UV radiation.[1] In the case of cw laser systems, the use of an angle or temperature tuned nonlinear crystal external to the dye laser cavity provides a tunable source of UV radiation of sufficient intensity for many spectroscopic applications. However, much higher UV powers can be obtained through intracavity second harmonic generation (ISHG). In earlier studies of ISHG emphasis was placed on obtaining maximum single frequency powers at specified wavelengths or broadband outputs tunable over short wavelength intervals ~300 nm.[2–9] In this paper the design and operation of a computer controlled, intracavity doubled, scanning cw dye ring laser is described. This laser system is the first to provide single frequency UV output powers of up to 10 mW with a FWHM linewidth of ~100 MHz continuously tunable over intervals of 3200 GHz in the 285–311-nm wavelength range and is suitable for use in a wide variety of spectroscopic applications.

In the present study, the computer controlled ring laser described previously[10] was modified to include a third beam focus of 45-μm radius ($1/e$) within the cavity. The new cavity configuration is shown schematically in Fig. 1. The configuration is designed to compensate for the crystal, dye jet, and mirror astigmatism[11] and provide sufficient space for intracavity hardware. Detailed calculations[12] show that for a Brewster-cut SHG crystal with an optical path length of 15 mm, compensation is achieved at a relatively small angle of incidence on each mirror, ~3.7°, and that the cavity is stable over an appreciable range of mirror separations. Laser tuning is accomplished by use of a standard three-element birefringent filter and two etalons, all under computer control to obtain continuous scanning. A small visible output (~200 mW) is extracted at mirror $M4$ for diagnostic purposes. When operating with Rh6G, unidirectional single-mode (40-MHz linewidth) intracavity powers of 7–10 W are obtained with 5 W of 514.5-nm pump radiation. The intracavity power is limited primarily by the insertion losses associated with the Faraday rotator (Hoya FR-5 glass, 9-mm optical path length) and air spaced etalon (30-GHz, FSR ~2.5 finesse). The optical rotation of ~10° produced by the Faraday rotator is considerably greater than that required to ensure stable unidirectional operation.[13] However, the thickness of the required reciprocal c-axis quartz rotator is 0.5 mm and is such that this element can also serve as an intracavity etalon. Thus, although the thickness of the Faraday rotator could be reduced, thereby reducing losses associated with this element, this requires the introduction of an additional intracavity element. For applications requiring higher powers with modest linewidth (40 GHz), the etalons and Faraday isolator are removed. An external mirror is then used to ensure quasi-unidirectional operation.[13] In this configuration fundamental circulating powers >25 W are attained. Frequency doubling is accomplished using a nonlinear crystal located as shown in Fig. 1. The second harmonic output emerges through mirror $M5$, which is highly reflecting in the visible but 80% transmissive in the UV.

Ammonium dihydrogen arsenate (ADA) was chosen as the nonlinear medium since this material permits noncritical 90° temperature tuned phase matching over most of the useful tuning range of Rh6G. However, for comparison purposes, experiments were also conducted using a 65° z-cut ammonium dihydrogen phosphate (ADP) crystal. The fundamental confocal parameter

The authors are with Rice University, Departments of Electrical Engineering and Space Physics & Astronomy, Houston, Texas 77001.

Received 5 January 1980.
0003-6935/80/121980-04$00.50/0.

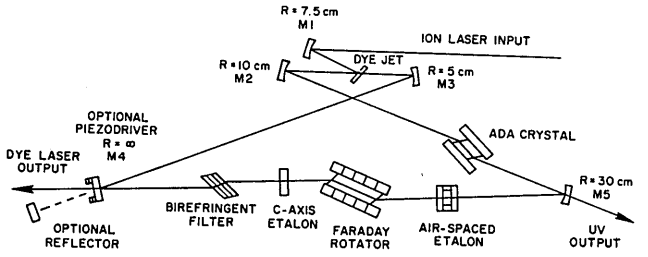

Fig. 1. Schematic of cw ring dye laser spectrometer with intracavity SHG.

at the crystal, $b \sim 3$ cm, suggests an optimum SHG crystal length of ~10 cm.[14] However, consideration of absorption and thermal effects in the crystal dictates the use of crystals of shorter lengths.[6] Substantial reduction of the confocal parameter to accommodate shorter crystals was precluded by cavity size requirements and the strong coupling between the dye jet and crystal focal radii.

Four ADA crystals with cross sections of 5 × 5 mm and optical path lengths of 15, 15, 20, and 30 mm were employed in this work. The 15- and 20-mm crystals had Brewster-cut entrance and exit faces to minimize reflection losses and to maximize the fundamental power density in the cavity and hence the UV output. However, since the fundamental and second harmonic beams orthogonally polarized in type I phase matching, the Brewster-cut exit face transmits only 83% of the UV generated in the crystal. An attempt was made to avoid this loss by using a crystal (30 mm long) with entrance and exit faces normal to the incident beam. To reduce reflection losses antireflection coatings must be employed. However, such coatings applied directly to ADA isomorphs are extremely susceptible to thermal damage, and the coatings were therefore applied to fused silica windows that were then attached to the crystal with an index matching fluid. In addition to having a suitable refractive index, this fluid was required to be compatible with the water soluble ADA crystal, transparent at both the fundamental and second harmonic wavelengths and capable of withstanding the high power densities. Four materials (silicon oil, fluorocarbon FC-104, carbon tetrachloride, and an epoxy resin) were tried, and all were found to reduce second harmonic output due to deterioration under intense UV radiation and thermal defocusing. Thus, since substantial losses with normal incidence crystals could not be avoided, the use of Brewster-cut crystals appears preferable.

The absorption and optical quality of the nonlinear crystals were found to be extremely important in determining the tunable UV output powers obtained. However, the insertion losses associated with the highest quality nonlinear crystals were considerably less than those of the Faraday rotator or air spaced etalon. Surprisingly, crystals from different suppliers were found to degrade the performance of the dye laser by widely differing amounts. Aside from the reduction in power and wavelength coverage caused by the insertion losses, crystals of poor optical quality also introduced other deleterious effects including a reduction in the frequency stability of the laser and an interaction between crystal temperature and laser tuning.

The temperature and angle tuning characteristics of ADA were determined in a preliminary study using a separate pulsed dye laser system. The use of a low average power pulsed system avoids uncertainties caused by laser heating of the crystal.[7] Analysis of the temperature tuning data obtained for 90° phase matched SHG in ADA showed that for any crystal temperature T(°C) in the range from −40° to 100°C the corresponding phase matched fundamental wavelength (nm) is given to a good approximation (±0.2 nm) by

$$\lambda_m = 577.7 + 0.281T + 0.00055T^2. \quad (1)$$

In addition the angle tuning curve measured at 24°C was found to disagree by several nanometers with the curve calculated from single term Sellmeier approximations to the refractive index data of Winchell.[15] Therefore, revised Sellmeier constants for ADA have been calculated, normalized to the published index data,[15] and provide an excellent fit to the experimental angle tuning curve at 24°C for fundamental wavelengths from 584 to beyond 650 nm. These constants are presented in Table I.

Reliable and convenient temperature control of the nonlinear crystal is essential for stable temperature tuned ISHG. Figure 2 shows the second harmonic

Table I. Sellmeier Coefficients for Room Temperature Indices of ADA; Indices are given by $n^2 - 1 = 1/(A - B/\lambda^2)$.

	A	B
O Ray	0.69945	9051 nm^2
E Ray	0.78678	9740 nm^2

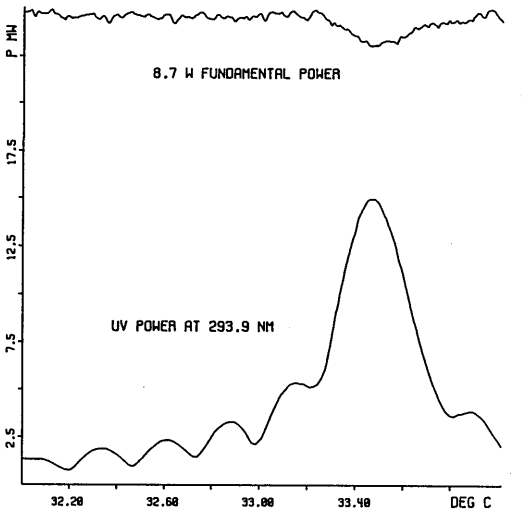

Fig. 2. Temperature dependence of SHG power in ADA at fixed wavelength of 293.9 nm.

power generated at a constant wavelength of 294 nm as the temperature of the ADA crystal is scanned smoothly through the phase matching temperature of 33.5°C. As can be seen, temperature control to ±0.05°C is required to maintain the second harmonic output within 5% of maximum. This control is accomplished over a 10–100°C temperature range with a specially designed compact crystal oven and an Artronix model 5301 temperature controller. This temperature controller is interfaced to the DEC PDP 11/V03 minicomputer through a Camac controlled stepping motor. The low noise and high resolution available with this technique make it preferable to a direct electrical interface.

The crystal temperature and the laser fundamental frequency are synchronized by the system software to provide constant UV output power during scanning. Each laser tuning element is calibrated with respect to frequency as detailed in Ref. 10. The crystal temperature at a given position of the oven controller stepping motor is calculated from the corresponding phase matching fundamental frequency, determined by maximizing second harmonic output power, and the temperature tuning polynomial of Eq. (1). This reference point is then used with the known characteristics of the oven controller to adjust the crystal temperature in synchronization with the fundamental frequency in the wavelength range of interest. In practice only one reference point is required for each UV spectral segment of 3200 GHz. No direct monitoring of the crystal temperature by the computer is necessary. Problems arising from the finite response time of the oven to changes in the temperature setting are eliminated in the system software.

With the laser configured as shown in Fig. 1, use of 5 W of pump light at 514.5 nm and a 15-mm ADA crystal yields stable second harmonic outputs of typically 10 mW at a FWHM linewidth of ~100 MHz. Operation in the broadband mode with the external feedback mirror initially yields output powers >30 mW. However, these higher powers were observed to decay rapidly, and stable output powers of ~20 mW were typically obtained. This reduction in output power probably results from a combination of thermal effects associated with UV absorption by the nonlinear crystal[6,7] and the fact that the crystal introduces a frequency-dependent loss in the cavity, which can suppress laser operation at the optimal phase matching wavelength by enhancing the relative gain of modes at either side of this wavelength.

When corrected for reflection losses a single-mode output power of 10 mW corresponds to the generation of 16 mW in the crystal. Under these conditions, since the intracavity fundamental power is ~7.5 W, the nonlinear conversion coefficient is $\sim 3 \times 10^{-4}$ W^{-1}. This result, in conjunction with the theory of Boyd and Kleinman,[14] allows the nonlinear susceptibility of ADA to be estimated as $d_{36} \sim 5 \times 10^{-13}$ m · V^{-1} ($\sim 1 \times 10^{-9}$ esu). This same value was obtained in similar measurements using the 30-mm normal incidence ADA crystal. Since the laser cavity is astigmatically compensated for a Brewster-cut crystal, this result suggests

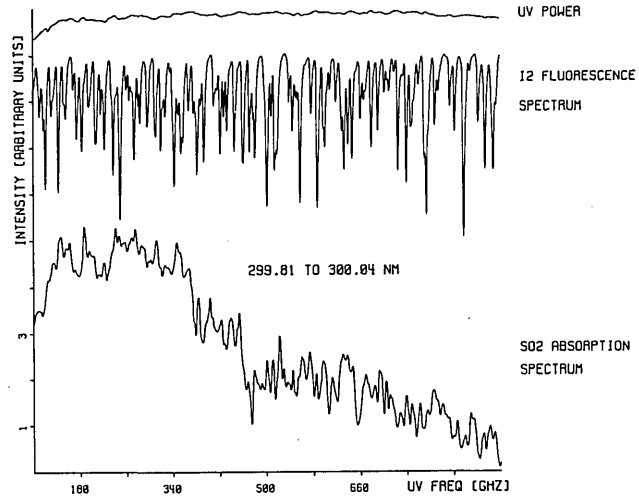

Fig. 3. Typical long-range single frequency scan (800 GHz) under computer control of UV absorption spectrum of SO_2 (cell length, 25 cm; cell pressure, ~5 Torr). Also shown for reference is fluorescence spectrum of I_2 obtained simultaneously using visible output of the spectrometer.

that variations in astigmatic distortion of the fundamental beam do not substantially reduce second harmonic conversion efficiency in the present system, although the performance of the dye laser is somewhat degraded. A UV output of 6 mW (at 12 W of intracavity power) was obtained by use of an ADP crystal of 25-mm length from which the value $d_{36} \sim 5 \times 10^{-13}$ m · V^{-1} may be inferred in good agreement with the generally accepted value.

The usefulness of the laser system as a spectrometer was demonstrated by observing the absorption spectrum of SO_2. Figure 3 shows the SO_2 spectrum (5 Torr) taken in a single continuous scan at a rate of 6 GHz/sec. The resolution of this spectrum is limited to ~170 MHz in the visible by the longitudinal cavity mode spacing. Also shown is a fluorescence spectrum of I_2 acquired simultaneously, as a wavelength reference, using the fundamental output of the laser.

We would like to thank C. R. Pollock, J. V. V. Kasper, and D. Frolich for many helpful discussions and E. D. Dahl for substantial contributions to the preliminary ADA survey. This work was supported by the Department of Energy, the National Science Foundation, and the Robert A. Welch Foundation.

References

1. S. Blit, E. G. Weaver, F. B. Dunning, and F. K. Tittel, Opt. Lett. **1**, 58 (1977); Appl. Opt. **17**, 721 (1978).
2. C. Gabel and M. Hercher, IEEE J. Quantum Electron. **QE-8**, 850 (1972).
3. D. Frolich, L. Stein, H. W. Schroder, and H. Welling, Appl. Phys. **11**, 97 (1976).
4. A. I. Ferguson, M. H. Dunn, and A. Maitland, Opt. Commun. **19**, 10 (1976).
5. H. W. Schroder, L. Stein, D. Frolich, B. Fugger, and H. Welling, Appl. Phys. **14**, 377 (1977).
6. A. I. Ferguson and M. H. Dunn, IEEE J. Quantum Electron. **QE-13**, 751 (1977).

7. A. I. Ferguson and M. H. Dunn, Opt. Commun. **23,** 177 (1977).
8. C. E. Wagstaff and M. H. Dunn, J. Phys. D: **12,** 355 (1979).
9. S. M. Jarrett and J. F. Young, Opt. Lett. **4,** 176 (1979).
10. C. R. Pollock, J. Kasper, G. K. Ernst, W. E. Ernst, S. Blit, and F. K. Tittel, Appl. Opt. **18,** 1907 (1979).
11. H. W. Kogelnik, E. P. Ippen, A. Dienes, and C. V. Shank, IEEE J. Quantum Electron. **QE-8,** 373 (1972).
12. Details of cavity dimensions and parameters are available upon request, C. M. Marshall, M.Sc. Thesis, Rice U. (1980).
13. T. F. Johnston, Jr. and W. Proffitt, IEEE J. Quantum Electron. **16,** April (1980).
14. G. D. Boyd and D. A. Kleinman, J. Appl. Phys. **39,** 3597 (1968).
15. A. N. Winchell, *Microscopic Characters of Artificial Minerals* (Wiley, New York, 1931).

Books *continued from page 1968*

this field, coupled with semiempirical calculations will yield in the future all the information needed." Most of the field hands would, I believe, regard this assessment of available semiempirical methods as decidedly optimistic.

Some corrections not included in the calculations tabulated here, such as relativistic effects, configuration interaction, and term dependence, are of major importance in a wide range of problems now being worked on. The authors might well have pointed out with more emphasis and detail the limitations of the approximation they used. These tables will probably be consulted fairly often by some atomic scientists, and I would guess that a larger group will find them occasionally useful.

WILLIAM C. MARTIN

Atomic Spectra and Radiative Transitions. By IGOR I. SOBELMAN. Springer-Verlag, New York, 1979. 318 pp. $35.00.

In the relatively small space of just over 300 pages, this book presents a wealth of information about the quantum mechanics of free atoms. The emphasis is on the use of Racah's tensorial methods to calculate atomic properties. Therein lies its strength; probably no other book on the subject covers such a wide range of topics from the standpoint of tensor algebra. After concise reviews of the hydrogen atom and the systematics of atomic energy levels, the author treats at length the theory of angular momentum, the calculation of energy levels in multielectron atoms, hyperfine structure, the Stark effect, the Zeeman effect, and radiation processes.

Some of the specific subjects covered are not often found in textbooks. The discussion of *jl,* intermediate, and other types of coupling is noteworthy in this respect. Although the development is generally highly mathematical, a number of useful numerical tables are included. Those for the ground terms and ionization energies of neutral atoms (3.1), fractional parentage coefficients (5.1–5.16), photoionization cross-section parameters (9.3), transition probabilities for hydrogen (9.4–9.5), transition probabilities calculated in the Coulomb approximation (9.6–9.7), and experimental oscillator strengths (9.8) are the most extensive. Some of the tables might be more descriptively captioned, but this is a minor drawback. In Table 3.1 the question marks given for the ground terms of several atoms should be removed. These states are now all well established.

More importantly, in Table 5.8 all the coefficients of fractional parentage for states of d^6 based on states of d^5 with seniority $v' = 3$ should be reversed in sign. This phase problem appears to be due to omission of the factor $(-1)^{(v'-1)/2}$, which is required when Eq. 5.35 is used to obtain CFPs for states of configurations of the type l^{2l+2}; that is, for configurations just past the half-filled shell. In Table 5.3 the coefficient of fractional parentage $(p^4\ ^1D\{p^3[^2D]p\ ^1D)$ should be $-[3/4]^{1/2}$ rather than $+[3/4]^{1/2}$.

Quite a few applications of the theory are given. However, many are dated. No mention is made of effective interactions (such as the Trees $\alpha L(L+1)$ correction) that have come to play such an important role in the interpretation of atomic spectra. Also, the list of references is inadequate; a total of only thirty-two works are cited. Certainly, Nielson and Koster's *SPECTROSCOPIC COEFFICIENTS FOR THE p^n, d^n, AND f^n CONFIGURATIONS* and *THE 3-j AND 6-j SYMBOLS,* by Rotenberg, Bivins, Metropolis, and Wooten, would be of interest to those seeking to apply the theory. For information about spectra of rare-earth elements, Wybourne's *SPECTROSCOPIC PROPERTIES OF RARE EARTHS* might well have been mentioned. (*ATOMIC ENERGY LEVELS—THE RARE EARTH ELEMENTS,* by Martin, Zalubas, and Hagan, is now also available in this area.) The chapter on hyperfine structure contains no references—not even to the classic *NUCLEAR MOMENTS,* by Kopfermann.

Much of the present material was given originally in the earlier Sobelman volume *INTRODUCTION TO THE THEORY OF ATOMIC SPECTRA,* the English version of which was published by Pergamon Press in 1972. According to the author, the present text is intended as the first part of a two-volume presentation of the theory of atomic spectra, atomic radiative transitions, excitation of atoms, and spectral line broadening. For those who already own the earlier volume, the addition of the present book is probably not necessary. For those who do not, it is nearly a must.

JOSEPH READER

Optical Investigations of the Emission of the Atmosphere, Aurorae, and Noctilucent Clouds Aboard the Orbiting Scientific Station Salyut-4. Edited by L. YA. RIIVES and A. G. NIKOLAEV. Academy of Sciences of the Estonian S.S.R., Tallin, 1977. 176 pp. 1 R. 97 kop.

This book describes the optical investigations carried out from the Salyut-4 space station by astronauts Gubarev and Grechko, who manned the station in January and February 1975, and Klimuk and Sevastyanov, who manned it from May to July 1975. The volume consists of ten articles, each with multiple authorship, devoted to different aspects of the observations. Each article is accompanied by twenty to thirty references, and there is a total of thirty-three figures.

The first article outlines the general program of optical investigations carried out aboard Salyut-4. An overall picture is given of the atmosphere as observed from space. The night and twilight horizons are discussed as well as the daytime horizon. The spatial structure of emitting regions is described. An account is given of the radiometric, photographic, and spectrometric methods employed together with a brief summary of the results.

The next paper is devoted to auroral observations and commences with a brief summary of the literature on the space–time distribution of optical auroral emission and on stable auroral red arcs. The results of visual observations of aurorae from Voskhod, Soyuz-9, Soyuz-15 and Salyut are given. Visual observations from Salyut-4 of aurorae at the southern auroral oval to the south of Australia are presented.

The third article describes the visual and photographic observations of noctilucent clouds made aboard Salyut-4. Twenty-seven observations were made from space, and some of these were simultaneously recorded by ground-based stations. Morphological structure and the multilayered character of the noctilucent cloud field are described. The cloud fields cover a belt at latitudes above 45°.

The next presentation gives a physical interpretation of the spectra of noctilucent clouds in the near infrared. Curves of the vertical brightness profile at a wavelength of $\lambda = 1.35\ \mu m$ are given, and these show that the radiometer can detect noctilucent clouds.

The fifth article discusses day and twilight O_2 emission at 1.25 μm obtained from vertical profiles of horizon brightness recorded by a four-channel near-IR radiometer.

continued on page 1995